Hindawi
Journal of Robotics
Volume 2024, Article ID 9785472, 1 page
https://doi.org/10.1155/2024/9785472

Retraction

Retracted: Design and Application of Electromechanical Control System Based on Computer Fault Tolerance Technology

Journal of Robotics

Received 23 January 2024; Accepted 23 January 2024; Published 24 January 2024

This article has been retracted by Hindawi following an investigation undertaken by the publisher [1]. This investigation has uncovered evidence of one or more of the following indicators of systematic manipulation of the publication process:

(1) Discrepancies in scope
(2) Discrepancies in the description of the research reported
(3) Discrepancies between the availability of data and the research described
(4) Inappropriate citations
(5) Incoherent, meaningless and/or irrelevant content included in the article
(6) Manipulated or compromised peer review

The presence of these indicators undermines our confidence in the integrity of the article's content and we cannot, therefore, vouch for its reliability. Please note that this notice is intended solely to alert readers that the content of this article is unreliable. We have not investigated whether authors were aware of or involved in the systematic manipulation of the publication process.

Wiley and Hindawi regrets that the usual quality checks did not identify these issues before publication and have since put additional measures in place to safeguard research integrity.

We wish to credit our own Research Integrity and Research Publishing teams and anonymous and named external researchers and research integrity experts for contributing to this investigation.

The corresponding author, as the representative of all authors, has been given the opportunity to register their agreement or disagreement to this retraction. We have kept a record of any response received.

References

[1] R. Wei, "Design and Application of Electromechanical Control System Based on Computer Fault Tolerance Technology," *Journal of Robotics*, vol. 2022, Article ID 7716900, 10 pages, 2022.

Hindawi
Journal of Robotics
Volume 2022, Article ID 7716900, 10 pages
https://doi.org/10.1155/2022/7716900

Research Article

Design and Application of Electromechanical Control System Based on Computer Fault Tolerance Technology

Rui Wei

College of Intelligent Science and Information Engineering, Xi'an Peihua University, Xi'an, Shaanxi 710125, China

Correspondence should be addressed to Rui Wei; weirui2020@peihua.edu.cn

Received 8 August 2022; Revised 14 September 2022; Accepted 19 September 2022; Published 5 October 2022

Academic Editor: Shahid Hussain

In order to improve the stability and control effect of the electromechanical control system, this paper designs the electromechanical control system combined with the computer fault-tolerant technology and proposes an electromechanical control signal processing algorithm. In order to improve the accuracy of the path loss calculation, according to Fresnel's law, this paper deduces the expression of the reflection coefficient of electromechanical control signal with the distance between the transmitting antenna and the receiving antenna as the main variable and then compares the path loss with the ground and the ceiling as the reflecting surface. In addition, in order to study the path loss, this paper selects different reflective materials to study their path loss under horizontal polarization and vertical polarization. The results show that under the vertical polarization, the path loss fluctuation is not large, and the agreement is higher than that of the horizontal polarization. The research results show that the electromechanical control system based on computer fault-tolerance technology proposed in this paper has stable performance and can play an important role in the control of electromechanical systems.

1. Introduction

With the continuous development of sliding mode control technology, it has a very strong control capability for nonlinear systems, time-delay systems, and model uncertain systems. Moreover, sliding mode variable structure control is gradually applied to various control fields as an effective comprehensive method. The sliding mode variable structure method has the advantages of strong robustness, good dynamic performance, and insensitivity to the perturbation of system model parameters, but the existence of chattering greatly affects the large-scale application of sliding mode variable structure control [1]. If the chattering is reduced to a certain extent while meeting the system performance requirements, the large-scale application of sliding mode variable structure control will become a possibility.

Fuzzy control theory has achieved very outstanding application results, especially in the field of intelligent home appliance control, fuzzy washing machines, fuzzy refrigerators, etc. emerge in an endless stream, but at present, fuzzy control still mainly draws on the control experience of experts, and people analyze its stability and robustness. It is still relatively difficult, and it is of great significance to be able to design a fuzzy controller with global stability [2]. It can be seen from the development process of control theory that no theory is perfect, and all have certain pertinence and limitations. For example, the PID control structure is simple and has strong control ability, but it is no longer suitable for nonlinear system control. Fuzzy control can simulate the control logic of experts, but it is completely controlled by fuzzy control, and its control rules will be very complicated [3]. Neural networks can achieve universal use of all controls through continuous learning, but the learning process is long; sliding mode control is suitable for almost all systems, but the chattering problem in practical applications greatly reduces the performance of the system. A single control theory is difficult to meet people's needs for system control, and two or more integrated control strategies are often used to obtain satisfactory results through the complementation of dynamic characteristics [4]. In recent years, fuzzy sliding mode control has achieved rapid development. Compared with traditional sliding mode, the robustness and

convergence speed of the system have been improved, and the system has higher steady-state accuracy near the switching surface [5]. The fuzzy sliding mode algorithm is designed according to the principles of real-time and robustness, which improves the speed of system leveling, reduces the chattering of the system, and reduces the impact of traditional PWM control on the hardware system [6].

For the study of electromechanical dynamics of power systems, the current method is usually to establish detailed mathematical models of dynamic components such as generators and loads and then construct system algebraic equations according to the system topology, using eigenvalue method, energy function method, or numerical methods such as time-domain simulation method to solve. Then, there are two methods to determine whether the system is in a steady state, one is to compare the obtained analytical solution with the relevant stability indicators [7]; the other is to specify the curve of system parameters changing with time to determine. However, with the interconnection of cross-regional power grids, thousands of generators and a larger number of busbars and components form a huge power grid system, making the modern power grid structure more and more complex and huge. If the method described above is still adopted, the calculation is so complicated that it is almost unsolvable due to the huge system, which makes it difficult to explain the propagation of electromechanical disturbances from a microscopic point of view [8]. Since the electromechanical dynamics of the power system mainly studies the angular velocity increment and the spatiotemporal distribution of the power increment, it is necessary to simplify the power system and look at the huge power system from a macro perspective. The power system continuum model describes the system as a continuum by simplifying the system model, ignoring the electromagnetic transients of the generator rotor and stator, and ignoring the reactive power transmission and voltage changes in the system [9]. The electromechanical disturbance is regarded as a kind of electromechanical wave, and the propagation of electromechanical disturbance in the macroscopic power system is analyzed from the perspective of wave. The continuum model of power system provides a new idea for studying the electromechanical dynamic characteristics of large-scale power system. Reference [10] established a continuum model of the electromechanical dynamics of the power system in order to study the electromechanical dynamics in the power system. Simplify the conditions first, make a series of assumptions for transmission lines and generators, deduce the constant coefficient linear wave equation about the propagation of electromechanical disturbances, give the propagation speed of electromechanical disturbances, and expound the reflection, static and static control of electromechanical control signals, and physical phenomena such as waves. Comparing the simulation and actual data, the 0.2 Hz low-frequency oscillation phenomenon on the Pacific tie line was explained from the perspective of electromechanical waves, and satisfactory results were obtained, which provided a new reference for the mechanism research of low-frequency oscillation [11]. Incorporating the Bessel function lines and exponents into the electromechanical dynamics, the electromechanical dynamic equivalence problem of $\Delta P - \Delta f$ is studied, and the problem that the frequency change in the power grid affects the propagation speed of electromechanical disturbances is discussed for the first time [12]. Reference [13] uses the incremental element model and continuously processes the inertial parameters of the generator to convert it into the form of a spatial density function. Based on this model, the attenuation characteristics and propagation velocity of electromechanical disturbances are deduced and calculated. The propagation velocity of the generator power angle measured by the synchrophasor measuring device is compared with the electromechanical disturbance velocity of the simulation system established by him, and the comparison results show that the two have a high degree of agreement. Reference [14] established a differential element model of a one-dimensional chain system by imitating the uniform transmission line. By studying the relationship between the transmission power of the transmission line and the electromagnetic power output by the generator, the limit of the generator swing equation was limited in the space distance. Solved, the electromechanical wave equation is derived. By studying the reflection properties of zero electromechanical control signal and characteristic impedance matching of electromechanical waves on boundary effects, a method of applying zero electromechanical control signal reflection decentralized control in the continuous model of power system is proposed. The controller designed by this method can well absorb the active disturbance power at the boundary [15]. Reference [16] transformed the geographical location in the actual power grid into a two-dimensional plane and transformed the original generator inertia coefficient and angular momentum from the spatial density function form into a continuous distribution by a Gaussian function. The electromechanical disturbance propagation equation including position parameters is deduced by this method, and the phenomena such as dispersion, transmission, and electromechanical control signal reflection in the disturbance propagation process are analyzed and discussed accordingly, and the global dynamics of the power system disturbance propagation process are studied. Reference [17] studied the propagation characteristics of electromechanical waves in the large power grid system, using the generator swing equation, carried out numerical simulation of the traditional generator discrete model, and compared the numerical solution of the continuum model with the discrete model, indicating that the continuous solution of the volume model can better fit the discrete model.

This paper combines the computer fault-tolerant technology to design the electromechanical control system, improve the intelligent control effect of the

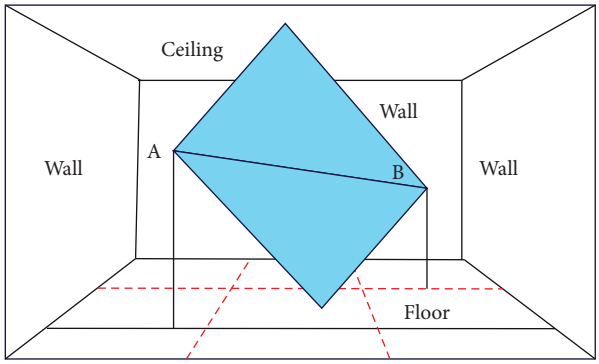

Figure 1: Layout of the test scene within the area.

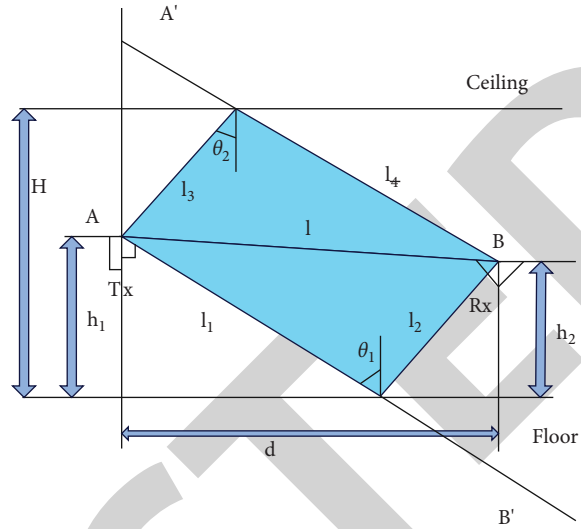

Figure 2: Geometrical optics analysis diagram.

electromechanical control system, and effectively promote the management effect of modern electromechanical equipment.

2. Electromechanical Control Signal Processing Algorithms

2.1. Research on Path Loss Based on Multipath Channel. From the electromagnetic theory, vertical polarization and horizontal polarization are relative to the horizontal plane. When the electric field vector is parallel to the ground, the linearly polarized wave at this time is called horizontally polarized wave. Conversely, when the electric field vector is perpendicular to the ground, the polarized wave is called vertically polarized wave. Therefore, the research on the reflection coefficient of the electromechanical control signal will also be based on the ratio of the horizontal polarization and the vertical polarization relative to the incident amount. Moreover, the reflection coefficient of the electromechanical control signal is determined by the incident angle, the polarization mode (horizontal and vertical) of the electric wave, and the relative permittivity of the medium. We set the incident angle of the radio wave as θ, and $\varepsilon_2/\varepsilon_1$ represents the relative permittivity of the radio wave incident from the material 2 to the material 1. For multipath channel propagation, the reflection coefficients of electromechanical control signals in horizontal polarization and vertical polarization modes are as follows:

$$R_{\mathrm{TE}}(\theta) = \frac{\cos\theta - \sqrt{(\varepsilon_2/\varepsilon_1) - \sin^2\theta}}{\cos\theta + \sqrt{(\varepsilon_2/\varepsilon_1) - \sin^2\theta}}, \tag{1}$$

$$R_{\mathrm{TM}}(\theta) = \frac{(\varepsilon_2/\varepsilon_1)\cos\theta - \sqrt{(\varepsilon_2/\varepsilon_1) - \sin^2\theta}}{(\varepsilon_2/\varepsilon_1)\cos\theta + \sqrt{(\varepsilon_2/\varepsilon_1) - \sin^2\theta}}. \tag{2}$$

Generally, the relative permittivity of air is 1, that is, $\varepsilon_1 = 1$, and substituting it into (1) and (2), the reflection coefficients of the horizontal and vertical electromechanical control signals are obtained as follows:

$$R_{\mathrm{TE}}(\theta) = \frac{\cos\theta - \sqrt{\varepsilon_r - \sin^2\theta}}{\cos\theta + \sqrt{\varepsilon_r - \sin^2\theta}},$$
$$R_{\mathrm{TM}}(\theta) = \frac{\varepsilon_r\cos\theta - \sqrt{\varepsilon_r - \sin^2\theta}}{\varepsilon_r\cos\theta + \sqrt{\varepsilon_r - \sin^2\theta}}. \tag{3}$$

Among them, σ is the conductivity of the electromechanical control signal reflecting surface material, λ is the wavelength, and $\varepsilon_r = \varepsilon_2$ is the relative permittivity of the electromechanical control signal reflecting material.

The size of the room selected in this experiment is 10m × 5m × 3m, and the ground and ceiling materials measured in the experiment are wood ($\varepsilon_r = 2$) and PVC ($\varepsilon_r = 4$), respectively. d represents the spacing between the transceivers. A and B represent the transceiver antenna respectively, and h_1 and h_2 represent the vertical distance between the antenna and the reflection surface of the electromechanical control signal, respectively. The test scene and geometric optical analysis are shown in Figures 1 and 2, respectively.

For the convenience of research, we set $c = h_1 + h_2$. There are the following geometric relationships:

$$\tan\theta = \frac{d}{c}, \tag{4}$$

$$\sin\theta = \frac{d}{\sqrt{d^2 + c^2}}, \tag{5}$$

$$\cos\theta = \frac{c}{\sqrt{d^2 + c^2}}. \tag{6}$$

Combining formulas (4), (5), and (6), the expression of the reflection coefficient of the electromechanical control signal about the transceiver spacing d can be obtained, where the reflection coefficient of the electromechanical control

signal in the horizontal polarization mode (R_{TE}) is as follows:

$$R_{\mathrm{TE}}(d) = \frac{(h_{1x}+h_{2x}) - \sqrt{(\varepsilon_r - 1)d^2 - \varepsilon_r (h_{4x}+h_{2x})^2}}{(h_{4x}+h_{2x}) + \sqrt{(\varepsilon_r - 1)d^2 - \varepsilon_r (h_{4x}+h_{2x})^2}}. \quad (7)$$

The reflection coefficient of the electromechanical control signal in the vertical polarization mode (R_{IM}) is as follows:

$$R_{\mathrm{TM}}(d) = \frac{\varepsilon_r (h_{1x}+h_{2x}) - \sqrt{(\varepsilon_r - 1)d^2 - \varepsilon_r (h_{1x}+h_{2x})^2}}{\varepsilon_r (h_{1x}+h_{2x}) + \sqrt{(\varepsilon_r - 1)d^2 - \varepsilon_r (h_{1x}+h_{2x})^2}}. \quad (8)$$

In the formula, the height sums obtained by different electromechanical control signal reflective surfaces are different, so there are:

$$h_{1x}+h_{2x} = \begin{cases} c, & \text{The reflecting surface is the floor,} \\ 2H - c, & \text{The reflecting surface is the ceiling.} \end{cases} \quad (9)$$

For a specific scenario, c and ε_r are constants. After the improvement, it can be obtained that the reflection coefficient of the electromechanical control signal of the electromagnetic wave is studied according to the distance between the sending and receiving, so as to avoid relying on the difficult incident angle to study the reflection of the electromechanical control signal and greatly reduce the measurement error.

When analyzing the multipath channel link loss model like geometric optics, the signal propagation situation becomes complicated due to the different placement of items in the area. At this time, the multipath propagation situation of the signal needs to be considered. Since the preconditions of the traditional path loss model are no longer satisfied, the two-warp model in the traditional sense cannot be considered alone. In most cases, for short-distance wireless links, the link can avoid obstacles encountered in the propagation process, so that the transmission and reception ends form line-of-sight (LOS) propagation. Therefore, in this paper, in order to effectively study the link loss of short-distance multipath propagation channels in the area, a deterministic model based on ray tracing can be used. The path loss of the short-distance wireless link in the area can be expressed as follows:

$$\mathrm{PL} = \frac{(4\pi/\lambda)^2}{G_r G_t \left| \left(e^{-j2d_d/\lambda}/l_d\right) + R_g \left(e^{-j2\pi_g/2}/l_g\right) + \sum_t R_r \left(e^{-j2\pi d_t/\lambda}/l_t\right) \right|^2}. \quad (10)$$

Among them, λ is the free space wavelength, G_r is the antenna gain of the receiving antenna, G_t is the antenna gain of receiving array, the value of the antenna gain is related to the design of the short-distance wireless transceiver antenna, and the specific value is affected by the printed board antenna. R_g and R_f are the reflection coefficient of the electromechanical control signal of the ground and the reflection coefficient of the electromechanical control signal of the ceiling, respectively. It should be noted that, in formula (10), the first two items are mandatory, but for the corridor environment in the area, the reflection paths of electromechanical control signals on the ceiling and wall must be added. For outdoor streets, only the direct path and the ground emission path can be selected.

This time, the three-path method is used to characterize the loss of short-distance wireless links in the area. These three paths are the direct path, the reflection path of the electromechanical control signal on the ground, and the emission path of the ceiling, and then the formula (10) can be rewritten as follows:

$$\mathrm{PL} = \frac{(4\pi/\lambda)^2}{G_r G_t \left| \left(e^{-j2\pi_d/\lambda}/l_d\right) + R_g \left(e^{-j2\pi_g/\lambda}/l_g\right) + R_f \left(e^{-j2\pi\pi_f/\lambda}/l_f\right) \right|^2}. \quad (11)$$

Among them, l_f is the reflection path length of the electromechanical control signal of the ceiling. The length of the traditional electromechanical control signal reflection path is mainly obtained by the incident angle which is difficult to measure, while this model can be determined by the spatial position of the transceiver antenna, that is, the distance d of the transceiver relative to the projection of the electromechanical control signal reflection surface. Since the room height H is set, there are:

$$l_x = \sqrt{l_d^2 - (h_{1x}+h_{2x})^2 + (h_{1x}+h_{2x})^2}. \quad (12)$$

Among them, the corresponding direct l_d, ground l_g, and ceiling l_f reflection path lengths of electromechanical control signals are, respectively:

$$\begin{cases} l_d = d, \\ l_g = \sqrt{l_d^2 - (h_1 - h_2)^2 + (h_1 + h_2)^2} = \sqrt{l_d^2 + 4h_1h_2}, \\ l_f = \sqrt{l_d^2 - (h_1 - h_2)^2 + [2H - (h_1 + h_2)]^2} = \sqrt{l_d^2 + 4h_1h_2 + 4H[H - c]}. \end{cases} \quad (13)$$

In general, the link loss of multipath channel propagation in the area is also a kind of channel model in the area. In order to have a good understanding of the link loss of multipath channel propagation in the area, the empirical model expression is generally widely used, and the formula is as follows:

$$\overline{L}(d) = L(d_0) + 10 \cdot \mathrm{nlg}(d/d_0). \quad (14)$$

In the formula, $\overline{L}(d)$ is the value of the average link loss when the distance between the sending and receiving ends is d, and $L(d_0)$ is the value of the average path loss at d_0 at the reference distance when m is free space. In the case of the area, $d_0 = 1\mathrm{m}, \lambda$ is generally taken, m is the working wavelength of the radio wave, and n is the link loss index, which represents the change of the path loss (approximately equal to 2 in free space). The path loss in free space environment can be expressed as follows:

$$L(d_0) = 20\lg(4\pi d_0/\lambda). \quad (15)$$

2.2. Numerical Results and Analysis. In the case of different materials for the reflection surface of the electromechanical control signal, the variation of the reflection coefficient of the electromechanical control signal of the vertical polarization (R_{TM}) and the horizontal polarization (R_{TE}) with the transmission and reception distance d is shown in the figure. Here, we take h = 20cm. The measured ground material and ceiling material are wood ($\varepsilon_r = 2$) and PVC ($\varepsilon_r = 4$), respectively, and the frequency of working in the millimeter wave band is set to 60 GHz.

It can be seen from Figure 3 that the reflection coefficient $R_{7M} < 0$ of the electromechanical control signal in the horizontal polarization mode decreases with the increase of the transceiver distance d, and finally approaches −1. At the same sending and receiving distance d, by comparing the electromechanical control signal reflective surface materials (wood and PVC), it is found that the greater the relative permittivity of the electromechanical control signal reflective surface material, the smaller the absolute value of the electromechanical control signal reflection coefficient. Among them, the absolute value of the reflection coefficient of the electromechanical control signal of the PVC material is the largest, and the absolute value of the reflection coefficient of the electromechanical control signal of the wood material is the smallest.

It can be seen from Figure 4 that in the vertical polarization mode, with the increase of the transceiver distance d, the reflection coefficient of the electromechanical control signal changes from a positive number to a negative number after passing through the origin 0, and finally approaches −1. The incident angle θ_B when passing through the origin 0 is the Brewster Angle. At this time, D is the distance between sending and receiving, which can be calculated according to formula (8):

$$D = c \cdot \sqrt{\varepsilon_r^*}. \tag{16}$$

When the distance between sending and receiving is $d > D$, the reflection coefficient of electromechanical control signal is negative. When the distance between sending and receiving is $d < D$, the reflection coefficient of electromechanical control signal is positive. In this case, the reflection coefficient of the electromechanical control signal of the electromechanical control signal reflection surface material will also be affected by D at the position of crossing point 0. When $d > D$, $R_{TE} > 0$, under the same distance between sending and receiving, the value of the reflection coefficient of the electromechanical control signal of the PVC material is the largest, and the value of the reflection coefficient of the electromechanical control signal of the wood material is the smallest. When $d < D$, $R_{IE} < 0$, under the same distance between sending and receiving, the absolute value of the reflection coefficient of the electromechanical control signal of the PVC material is the smallest, and the absolute value of the reflection coefficient of the electromechanical control signal of the wood material is the largest.

It can be seen from Figure 4 that the vertical distance between the transceiver antenna and the ground and ceiling can be changed, but as long as the distance between the transceiver antenna d and c remains unchanged, the reflection coefficient of the electromechanical control signal remains unchanged at this time. According to equation (7) and equation (8), the reflection coefficient of electromechanical control signal can be determined by the distance between sending and receiving d; thus, avoiding the difficulty in determining the reflection coefficient of electromechanical control signal by measuring the incident angle θ. Under the condition of using the link loss model, a new calculation expression can be obtained, which greatly improves the calculation accuracy.

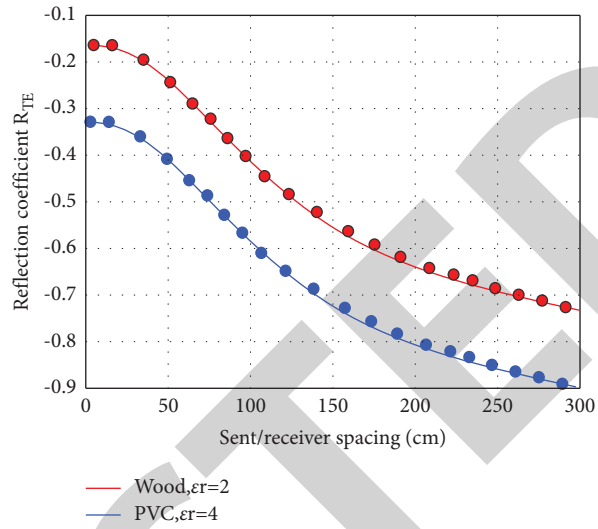

Figure 3: Reflection coefficient of electromechanical control signal under horizontal polarization.

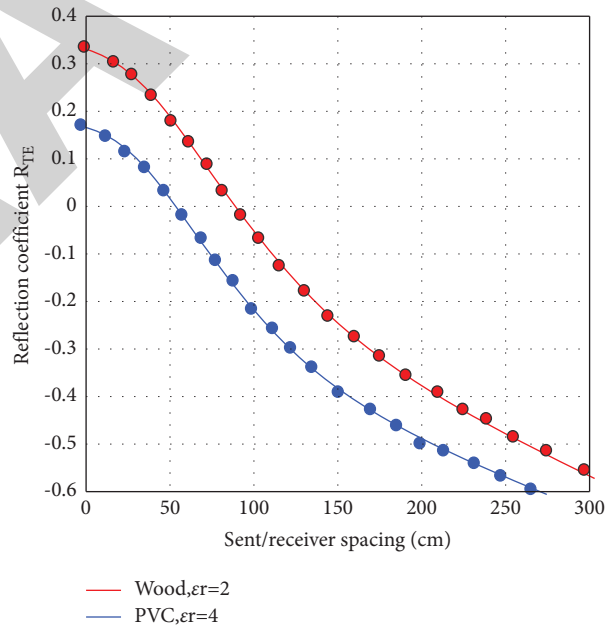

Figure 4: Reflection coefficient of electromechanical control signal in vertical polarization mode.

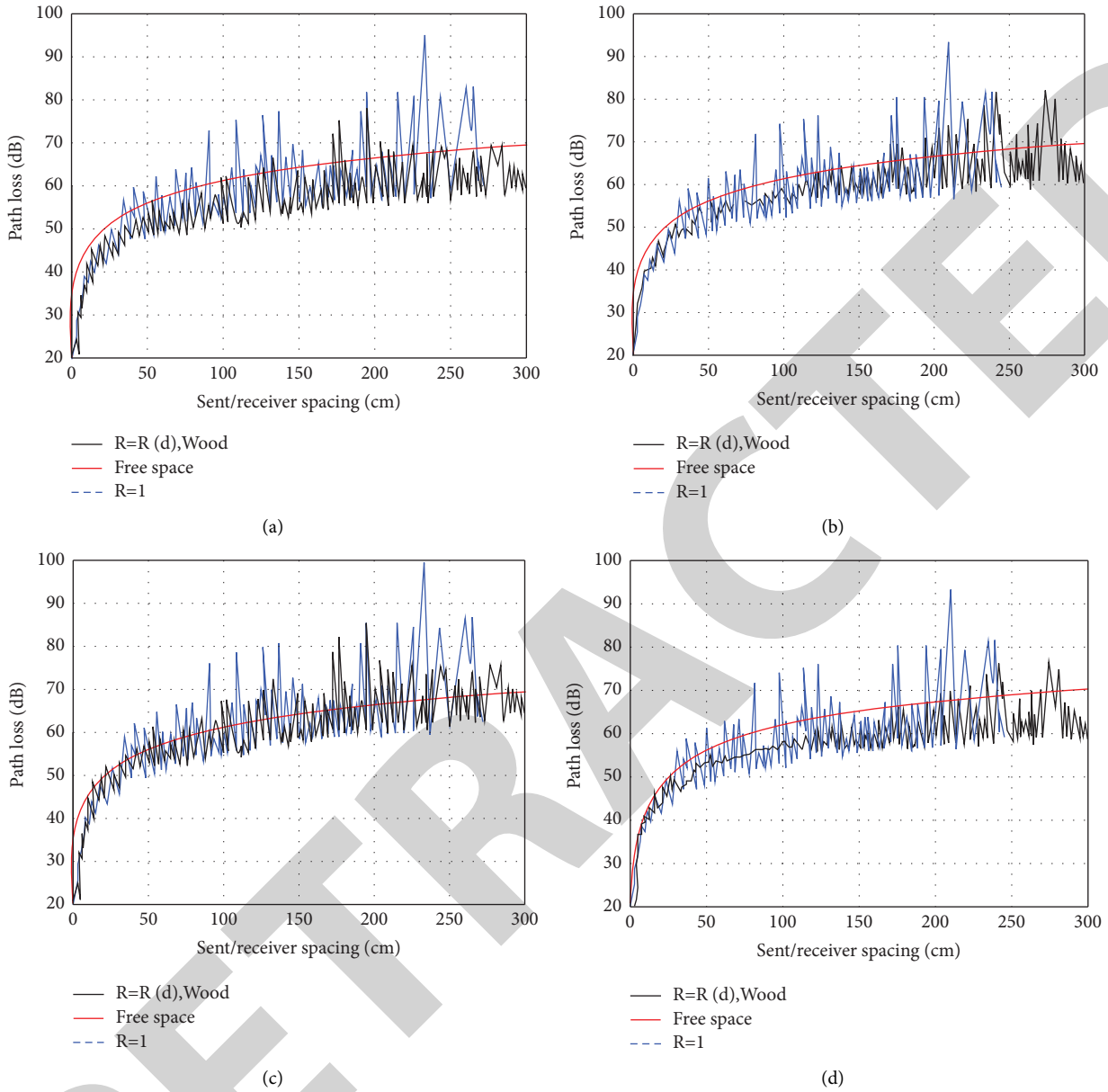

Figure 5: Waveform diagram. (a) Comparison of path loss under horizontal polarization, wood ground, $R = -1$, free space. (b) Comparison of path loss under vertical polarization, wood ground, $R = -1$, free space. (c) Comparison of path loss under PVC ceiling, $R = -1$, free space (horizontal). (d) Comparison of path loss under PVC ceiling, $R = -1$, free space (vertical).

For the convenience of research, under the traditional two-path model, the reflection coefficient of the electromechanical control signal is usually set to a constant (usually set to −1). Therefore, in order to facilitate the study of the difference between the multipath model and the two-path model, the reflection coefficient of the electromechanical control signal is still assumed to be −1 for the multipath model, and the vertical distance between the transmitting antenna and the receiving antenna to the ground is 20 cm. The path loss of different electromechanical control signal reflective surface materials (wood and PVC board) under different polarization modes (vertical and horizontal), the two-path model, and the path loss in free space are compared as shown in Figure 5.

As shown in Figure 5, from the overall waveform point of view, the value of the multipath link loss varies with the transmission and reception spacing. There will be multiple peaks and troughs at different transmission and reception distances; thus, forming multiple maximum and minimum values. From the perspective of the polarization mode, according to the knowledge of electromagnetic theory, the polarization current has a great influence on the propagation of the radio signal, and the intensity of the influence of different polarization modes on the signal propagation is also different. The main reason is that the ground is a conductor and does not generate polarized currents, resulting in the electromagnetic signal not rapidly attenuating. Therefore, compared with the path loss under the

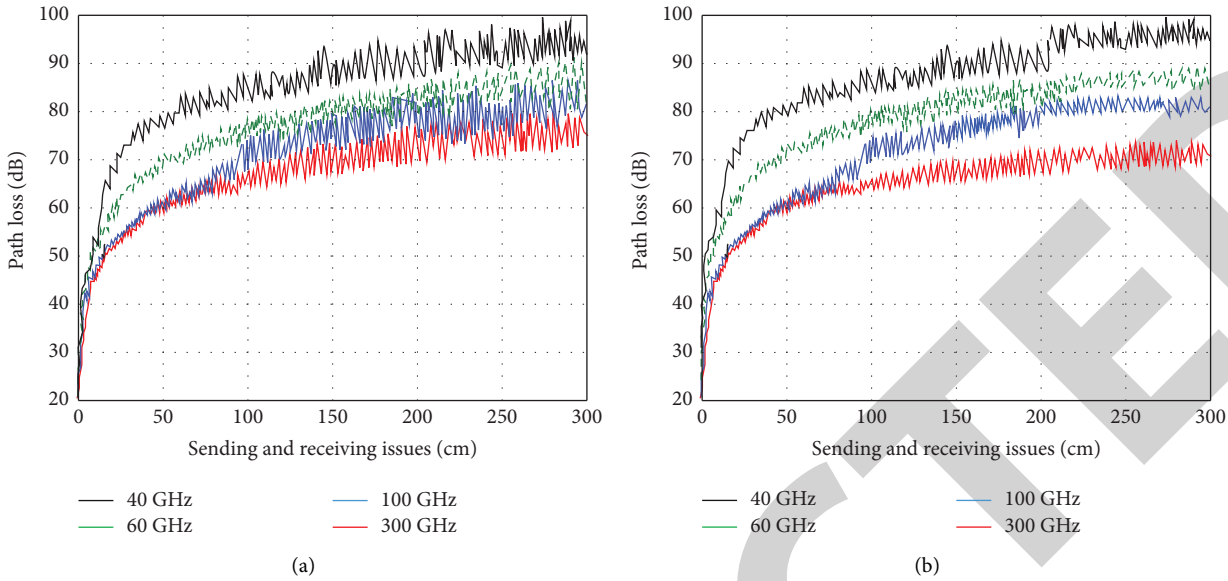

Figure 6: Comparison of path loss at different frequencies. (a) Comparison of path loss at different frequencies (horizontal). (b) Comparison of path loss at different frequencies (vertical).

horizontal polarization, since the polarization current will not be generated under the vertical polarization, the distance between the sending and receiving distance is 10 cm-100 cm. Moreover, the path loss under the vertical polarization is relatively stable, and there is no large fluctuation. On the contrary, there is a large fluctuation in the same distance range under the vertical polarization.

For regional multipath channel models, the difference between frequency sizes is also an important factor affecting path loss. In order to effectively analyze the influence of frequency on path loss, the path loss under different polarizations and frequencies is simulated by MATLAB. Taking the wood floor as the research object, the vertical distance from the antenna to the ground is set to 30 cm, and the four frequencies of 40 GHz, 60 GHz, 100 GHz, and 300 GHz are studied. The specific simulation diagrams are shown in Figure 6.

As can be seen from Figure 6, on the whole, with the increase of the transceiver spacing, there is no obvious difference between the path loss trends at these four different frequencies. The fluctuation range of the path loss in the entire transmission and reception distance is not large, and there is no trend of steep increase or decrease. From the perspective of the changing spacing range, whether it is horizontal polarization or vertical polarization, when the transmitting and receiving spacing changes in the range of 0-50 cm, the path loss increases faster. However, in the range of 50-300 cm, the variation range of the path loss is relatively stable. It can be seen from the comparison of the two polarization modes that when the transmission and reception distance is in the range of 50 cm-10 cm, the path loss under vertical polarization is relatively stable, and the range of amplitude variation is small. The main reason is that when the electromagnetic wave propagates in the horizontal polarization mode, the polarization current will be affected by the existence of the ground impedance, so that the electromagnetic signal will be attenuated. In contrast, vertical polarization does not generate polarization current, so it does not generate large fluctuations.

Therefore, from the above analysis, the improved multipath transmission channel link model has general applicability. The factors affecting the path loss are mainly determined by the vertical distance between the antenna and the reflection surface of the electromechanical control signal and the material of the reflection surface of the electromechanical control signal. In vertical polarization or horizontal polarization, the path loss obtained at different frequencies is also different.

When analyzing the link loss of a wireless channel within an area, a linear equation in the form of $y = ax + p$ is generally used to represent the characteristic of the average link loss on the logarithmic coordinate. Therefore, the equation for the average link loss is described as follows:

$$\overline{L} = a \cdot \log_{10}(d/d_0) + p. \tag{17}$$

Comparing formulas (14) and (17), it is found that in the logarithmic coordinate system, the theoretical prediction result formula and the empirical model formula are consistent in form. Therefore, the slope of the fitted straight line is: $a = 10n$, from which the value of the average path loss n can be obtained. There is a linear relationship between the link loss index n and the logarithm of the sending and receiving distance d (base 10). After fitting the data obtained from the test, the slope of the fitted curve is the link loss index n.

3. Electromechanical Control System Based on Computer Fault Tolerance Technology

For the purpose of improving the reliability and security of computer systems, using the theoretical knowledge and

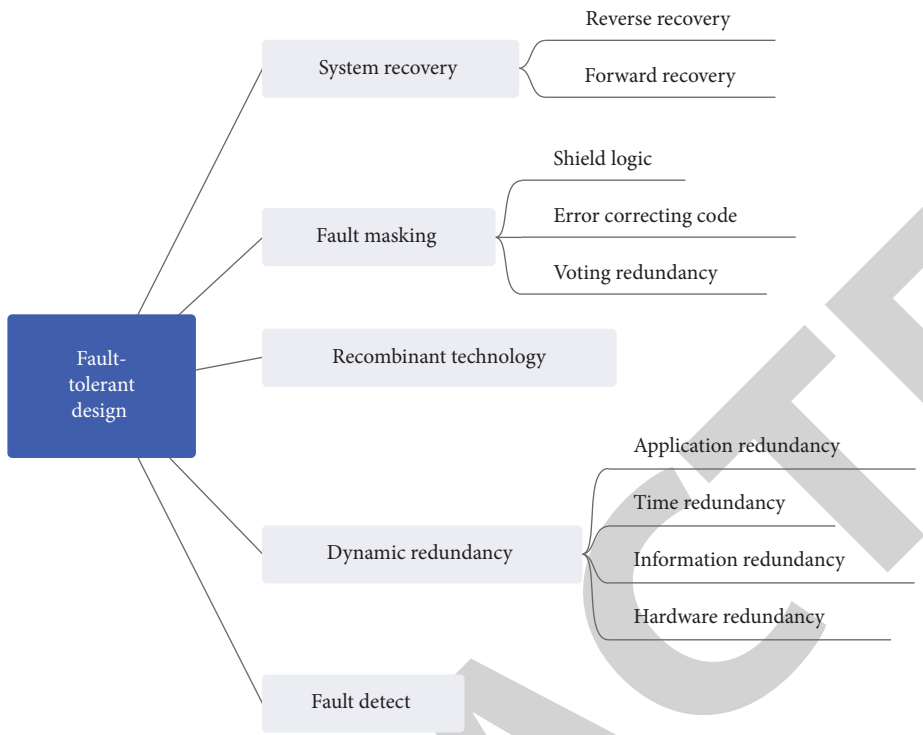

Figure 7: Fault-tolerant design method diagram.

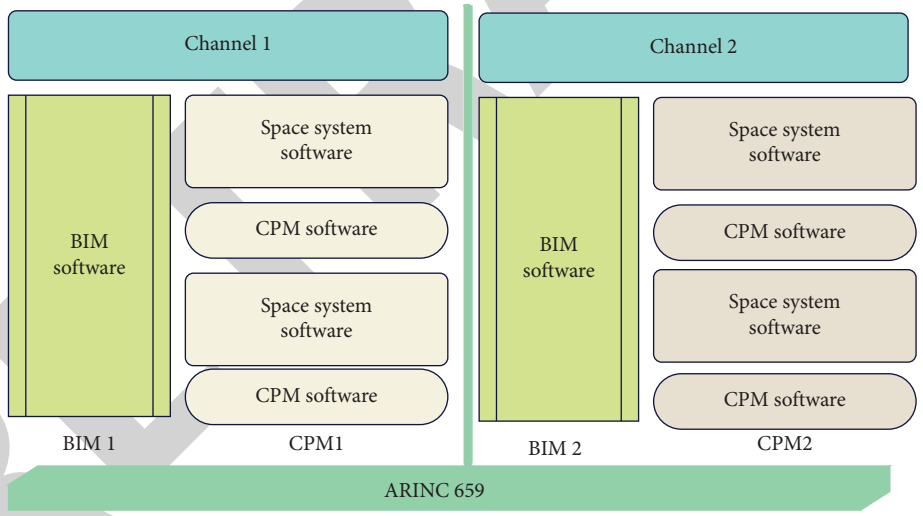

Figure 8: Structure diagram of comprehensive management computer software.

practical methods of fault-tolerant technology to formulate fault-handling strategies is the key to realizing system fault-tolerant design. The fault-tolerant design of the system is mainly realized through fault detection, fault shielding, dynamic redundancy, reorganization technology, and system recovery. The key steps of its fault-tolerant design are shown in Figure 7.

The integrated management computer system software is mainly composed of four parts: bus interface module software (BIM software), control management module software (CPM software), avionics system software (MMS software), and electromechanical system software (UMS software). The BIM module software is responsible for managing the collection of GJB289A bus, RS422 bus, and analog discrete quantity, etc. The CPM module software completes the redundancy management, input and output monitoring voting, task scheduling, and other work. The system structure is shown in Figure 8.

On the basis of the above research, the effect of the electromechanical control system based on computer fault-tolerance technology proposed in this paper is verified, and the control effect and system stability of the electromechanical system are counted, and the results shown in the following Figure 9 are obtained.

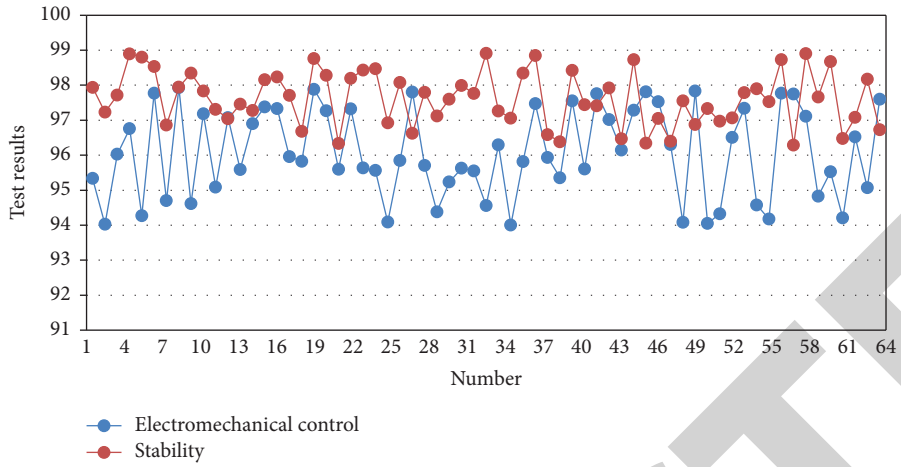

Figure 9: Verification of the effect of the electromechanical control system based on computer fault-tolerant technology.

It can be seen from the above research that the electromechanical control system based on the computer fault-tolerant technology proposed in this paper has stable performance and can play an important role in the control of electromechanical systems.

4. Conclusion

With the development of science and technology and control theory, the leveling system is developing towards intelligent automation and high precision, speed, and stability. Moreover, with the improvement and development of control objects and control devices, there are nonlinear, time-varying parameters, disturbances, unmodeled dynamics, mechanical resonance, and inconsistent responses of sensors to environmental factors in the system. This makes it difficult for the transfer function model and the state space model developed on this basis to accurately and comprehensively reflect the real characteristics of the object, and these unmodeled characteristics may lead to control failure in some specific cases. This paper combines the computer fault-tolerant technology to design the electromechanical control system to improve the intelligent control effect of the electromechanical control system. The research results show that the electromechanical control system based on computer fault-tolerance technology proposed in this paper has stable performance and can play an important role in the control of electromechanical systems.

Data Availability

The labeled dataset used to support the findings of this study is available from the corresponding author upon request.

Conflicts of Interest

The author declares that there are no conflicts of interest.

Acknowledgments

This work was supported by 2021 Project of Shaanxi Education Science "14th Five-year Plan": Research on the Construction of New Engineering Collaborative Education Mode Based on "Three Chains" Integration—A Case study of Computer Major (No.: SGH21Y0345).

References

[1] S. Zinchenko, V. Mateichuk, P. Nosov et al., "Use of simulator equipment for the development and testing of vessel control systems," *Electrical, Control and Communication Engineering*, vol. 16, no. 2, pp. 58–64, 2020.

[2] C. Gehrmann and M. Gunnarsson, "A digital twin based industrial automation and control system security architecture," *IEEE Transactions on Industrial Informatics*, vol. 16, no. 1, pp. 669–680, 2020.

[3] Y. Bichiou and H. A. Rakha, "Developing an optimal intersection control system for automated connected vehicles," *IEEE Transactions on Intelligent Transportation Systems*, vol. 20, no. 5, pp. 1908–1916, 2019.

[4] K. Eltag, M. S. Aslamx, and R. Ullah, "Dynamic stability enhancement using fuzzy PID control technology for power system," *International Journal of Control, Automation and Systems*, vol. 17, no. 1, pp. 234–242, 2019.

[5] K. Wang, E. Tian, J. Liu, L. Wei, and D. Yue, "Resilient control of networked control systems under deception attacks: a memory-event-triggered communication scheme," *International Journal of Robust and Nonlinear Control*, vol. 30, no. 4, pp. 1534–1548, 2020.

[6] M. Saraswat, K. Sharma, N. R. Chauhan, and R. K. Shukla, "Role of automation in energy management and distribution," *Journal of Scientific and Industrial Research*, vol. 79, no. 10, pp. 951–954, 2020.

[7] D. Xu, B. Wang, G. Zhang, G. Wang, and Y. Yu, "A review of sensorless control methods for AC motor drives," *CES Transactions on electrical machines and systems*, vol. 2, no. 1, pp. 104–115, 2018.

[8] M. Dumitrescu, "Marine industry automation systems simulation," *Scientific Bulletin "Mircea cel Batran" Naval Academy*, vol. 22, no. 2, pp. 7–13, 2019.

[9] H. Chen, B. Jiang, and N. Lu, "A multi-mode incipient sensor fault detection and diagnosis method for electrical traction systems," *International Journal of Control, Automation and Systems*, vol. 16, no. 4, pp. 1783–1793, 2018.

[10] B. Pratap and S. Purwar, "Real-time implementation of nonlinear state and disturbance observer-based controller for twin rotor control system," *International Journal of Automation and Control*, vol. 13, no. 4, pp. 469–497, 2019.

[11] Y. Yuan, H. Yuan, D. W. C. Ho, and L. Guo, "Resilient control of wireless networked control system under denial-of-service attacks: a cross-layer design approach," *IEEE Transactions on Cybernetics*, vol. 50, no. 1, pp. 48–60, 2020.

[12] S. J. Gambhire, D. R. Kishore, P. S. Londhe, and S. N. Pawar, "Review of sliding mode based control techniques for control system applications," *International Journal of Dynamics and Control*, vol. 9, no. 1, pp. 363–378, 2021.

[13] O. V. Kryukov, I. V. Gulyaev, and D. Y. Teplukhov, "Method for stabilizing the operation of synchronous machines using a virtual load sensor," *Russian Electrical Engineering*, vol. 90, no. 7, pp. 473–478, 2019.

[14] M. S. Jansi and M. K. Elaiyarani, "Iot based home automation system," *Turkish Journal of Computer and Mathematics Education (TURCOMAT)*, vol. 11, no. 3, pp. 2246–2253, 2020.

[15] W. Liang, M. Zheng, J. Zhang et al., "WIA-FA and its applications to digital factory: a wireless network solution for factory automation," *Proceedings of the IEEE*, vol. 107, no. 6, pp. 1053–1073, 2019.

[16] C. Wei, M. Benosman, and T. Kim, "Online parameter identification for state of power prediction of lithium-ion batteries in electric vehicles using extremum seeking," *International Journal of Control, Automation and Systems*, vol. 17, no. 11, pp. 2906–2916, 2019.

[17] T. A. Skouras, P. K. Gkonis, C. N. Ilias, P. T. Trakadas, E. G. Tsampasis, and T. V. Zahariadis, "Electrical vehicles: current state of the art, future challenges, and perspectives," *Cleanroom Technology*, vol. 2, no. 1, pp. 1–16, 2019.